

Analysis of the Time Fractional 2-D Diffusion-Wave Equation via Moving Least Square (MLS) Approximation

Elyas Shivanian¹

Published online: 15 September 2016
© Springer India Pvt. Ltd. 2016

Abstract In this paper, the time fractional two-dimensional diffusion-wave equation defined by Caputo sense for $(1 < \alpha < 2)$ is analyzed by an efficient and accurate computational method namely meshless local Petrov–Galerkin (MLPG) method which is based on the Galerkin weak form and moving least squares (MLS) approximation. We consider a general domain with Dirichlet boundary conditions further to given initial values as continuous functions. Meshless Galerkin weak form is adopted to the interior nodes while the meshless collocation technique is applied for the nodes on the boundaries of the domain. Since Dirichlet boundary condition is imposed directly therefore the general domains are also applicable easily. In MLPG method, the MLS approximation is usually used to construct shape functions which plays important rule in the convergence and stability of the method. It is proved the method is unconditionally stable in some sense. Two numerical examples are presented, one of them with the regular domain and the other one with non-regular domain, and satisfactory agreements are achieved.

Keywords Local weak formulation · Meshless local Petrov–Galerkin (MLPG) method · Moving least squares (MLS) · Diffusion-wave equation · Time fractional derivative

Introduction

The fractional derivative and fractional differential equations have been used to describe many phenomena in physics and engineering, such as boundary layer effects in ducts, allometric scaling laws in biology and ecology, colored noise, dielectric polarization, electromagnetic waves, electrode–electrolyte polarization, fractional kinetics, quantitative finance, quantum evolution of complex systems, power-law phenomenon in fluid and complex network, viscoelastic mechanics, etc. [1, 2]. On the other hand, an important class of fractional differential

✉ Elyas Shivanian
shivanian@sci.ikiu.ac.ir

¹ Department of Mathematics, Imam Khomeini International University, Qazvin 34149-16818, Iran

equations which has been studied widely in recent years is the time fractional diffusion-wave equation (FDWE). The time FDWE is obtained from the classical diffusion-wave equation by replacing the second-order time derivative term by a fractional derivative of order $(1 < \alpha < 2)$ [3]. Many of the universal electromagnetic, acoustic, mechanical responses can be described exactly by the FDWE [4]. It is also worth mentioning that fractional diffusion equation and diffusion wave equation have a lot in common, for example, they can behave like diffusion. To see some different kinds of fractional differential equations interest readers are referred to [5–7].

Strictly speaking, fractional diffusion-wave equation with damping is similar to the fractional Cattaneo equation where FDWE has more a term $f(x, t)$ rather than fractional Cattaneo equation. A considerable amount of papers have been appeared dealing with fractional diffusion-wave equation with damping (FDWE). It is well known that whereas diffusion equation describes a process, where a disturbance of the initial conditions spreads infinitely fast, the propagation velocity of the disturbance is constant for the wave equation. In a certain sense, the time-fractional diffusion-wave equation that is obtained from the diffusion equation by substituting the first derivative in time by the fractional derivative of order α , $1 < \alpha < 2$, interpolates between these two different behaviors.

The present paper considers the following time-fractional two-dimensional diffusion-wave equation of order $(1 < \alpha < 2)$:

$$\frac{\partial^\alpha u(\mathbf{x}, t)}{\partial t^\alpha} + \gamma_1 \frac{\partial u(\mathbf{x}, t)}{\partial t} = \gamma_2 \Delta u + f(\mathbf{x}, t), \quad \mathbf{x} \in \Omega \subseteq \mathbb{R}^2, t \in [0, T], \tag{1}$$

subject to compatible initial conditions

$$u(\mathbf{x}, 0) = \varphi(\mathbf{x}), \quad \frac{\partial u}{\partial t}(\mathbf{x}, 0) = \psi(\mathbf{x}), \quad \mathbf{x} \in \Omega, \tag{2}$$

and the boundary condition

$$u(\mathbf{x}, t) = g(\mathbf{x}, t) \text{ for } \mathbf{x} \in \Gamma = \partial\Omega, t \in [0, T], \tag{3}$$

where $\mathbf{x} = (x, y)$ is spatial variable, Γ the boundary of domain and, γ_1 and γ_2 are constants. Also, $f(\mathbf{x}, t)$ is source function with sufficient smoothness and, $\varphi(\mathbf{x})$, $\psi(\mathbf{x})$ and $g(x, t)$ are given continuous functions. Furthermore, in Eq. (1), the time-fractional derivatives are in the sense of Caputo which is defined by

$$D_t^\alpha F(t) = \begin{cases} \frac{1}{\Gamma(k-\alpha)} \int_0^t (t-\xi)^{k-\alpha-1} F^{(k)}(\xi) d\xi, & k-1 < \alpha < k, t > 0, \\ F^{(k)}(t), & \alpha = k. \end{cases} \tag{4}$$

In the case $\alpha = 2$, this equation is the telegraph equation, which governs electrical transmission in a telegraph cable [4]. This equation could also be characterized as a wave equation, governing wave motion in a string, with a damping effect due to the term $\frac{\partial u(\mathbf{x}, t)}{\partial t}$.

In the literature, several meshless weak form methods have been reported such as: Meshless methods based on weak forms such as the element free Galerkin (EFG) method [8, 9], meshless methods based on collocation techniques (strong forms) such as the meshless collocation method based on radial basis functions (RBFs) [10–23] and meshless methods based on the combination of weak forms and collocation technique [24–35].

The weak forms are used to derive a set of algebraic equations through a numerical integration process using a set of quadrature domain that may be constructed globally or locally in the domain of the problem. In the global weak form methods, global background cells are needed for numerical integration in computing the algebraic equations. To avoid

the use of global background cells, a so-called local weak form is adopted to develop the meshless local Petrov–Galerkin (MLPG) method [36–46].

In the last few years, several numerical methods have been proposed for solving FDWE, see [4] and Refs. therein. In Ref. [4], the authors have applied a collocation method based on the Legendre wavelets (LWs) to solve the 1-D form of the problem (1)–(3) and obtained good results. In this paper, we focus on the numerical solution of the Eqs. (1)–(3) (which is two-dimensional) using a kind of MLPG method which is based on the Galerkin weak form and moving least squares (MLS) approximation and achieve still satisfactory results. Two illustrative examples are given so that the one of them possesses regular domain and the other one enjoys non-regular domain.

The MLS Approximation Procedure

A meshless method uses a local approximation to represent the trial function with the values of the unknown variable at some nodal points. In the current paper, the moving least squares (MLS) approximation is used. Consider a sub-domain Ω_s , the neighborhood of a point \mathbf{x} and denoted as the support domain of the MLS approximation for the trial function at \mathbf{x} , which is located in the problem domain Ω (see Fig. 1). To approximate the function u in Ω_s , over a number of randomly located nodes $\mathbf{x}_i, i = 1, 2, \dots, n$, the Moving Least Squares approximant $u^h(\mathbf{x})$ of $u, \forall \mathbf{x} \in \Omega_s$, could be defined by

$$u^h(\mathbf{x}) = \mathbf{p}^T(\mathbf{x}) \mathbf{a}(\mathbf{x}) \quad \forall \mathbf{x} \in \Omega_s, \tag{5}$$

where $\mathbf{p}^T(\mathbf{x}) = [p_1(\mathbf{x}), p_2(\mathbf{x}), \dots, p_m(\mathbf{x})]$ is a complete monomial basis of order m , and $\mathbf{a}(\mathbf{x})$ is a vector containing coefficients $a_j(\mathbf{x}), j = 1, 2, \dots, m$ which are functions of the space coordinates \mathbf{x} . $p_j(\mathbf{x})$ is monomial in the space coordinate $x^T = [x, y]$, and m is the number of polynomial basis functions. The coefficient vector $\mathbf{a}(\mathbf{x})$ is discovered by minimizing a weighted discrete L_2 norm, defined as:

$$\begin{aligned} J(\mathbf{x}) &= \sum_{i=1}^n w_i(\mathbf{x}) [p^T(\mathbf{x}_i) \mathbf{a}(\mathbf{x}) - \hat{u}_i]^2 \\ &= [\mathbf{P} \cdot \mathbf{a}(\mathbf{x}) - \hat{\mathbf{u}}]^T \cdot \mathbf{W} \cdot [\mathbf{P} \cdot \mathbf{a}(\mathbf{x}) - \hat{\mathbf{u}}], \end{aligned} \tag{6}$$

where $w_i(\mathbf{x})$ is the weight function associated with the node i , with $w_i(\mathbf{x}) > 0$ for all \mathbf{x} in the support of $w_i(\mathbf{x})$, \mathbf{x}_i denotes the value of \mathbf{x} at node i , n is the number of nodes in Ω_s for which the weight functions $w_i(\mathbf{x}) > 0$, the matrices \mathbf{P} and \mathbf{W} are given as

$$\mathbf{P} = \begin{pmatrix} \mathbf{p}^T(\mathbf{x}_1) \\ \mathbf{p}^T(\mathbf{x}_2) \\ \vdots \\ \mathbf{p}^T(\mathbf{x}_n) \end{pmatrix}_{n \times m}, \quad \mathbf{W} = \begin{pmatrix} w_1(\mathbf{x}) & \dots & 0 \\ \dots & \dots & \dots \\ 0 & \dots & w_n(\mathbf{x}) \end{pmatrix}$$

and $\hat{\mathbf{u}}^T = [\hat{u}_1, \hat{u}_2, \dots, \hat{u}_n]$. Here, it should be noted that $\hat{u}_i, i = 1, 2, \dots, n$ in Eq. (6) are the fictitious nodal values, and not the nodal values of the unknown trial function $u^h(\mathbf{x})$ in general. The stationarity of J in Eq. (6) with respect to $\mathbf{a}(\mathbf{x})$ leads to the following linear system of equations between $\mathbf{a}(\mathbf{x})$ and $\hat{\mathbf{u}}$:

$$\mathbf{A}(\mathbf{x}) \mathbf{a}(\mathbf{x}) = \mathbf{B}(\mathbf{x}) \hat{\mathbf{u}}, \tag{7}$$

where the matrices $\mathbf{A}(\mathbf{x})$ and $\mathbf{B}(\mathbf{x})$ are given by

$$\mathbf{A}(\mathbf{x}) = \mathbf{P}^T \mathbf{W} \mathbf{P} = \mathbf{B}(\mathbf{x}) \mathbf{P} = \sum_{i=1}^n w_i(\mathbf{x}) \mathbf{p}(\mathbf{x}_i) \mathbf{p}^T(\mathbf{x}_i), \tag{8}$$

$$\mathbf{B}(\mathbf{x}) = \mathbf{P}^T \mathbf{W} = [w_1(\mathbf{x}) \mathbf{p}(\mathbf{x}_1), w_2(\mathbf{x}) \mathbf{p}(\mathbf{x}_2), \dots, w_n(\mathbf{x}) \mathbf{p}(\mathbf{x}_n)]. \tag{9}$$

The MLS approximation is well defined only when the matrix \mathbf{A} in Eq. (7) is non-singular. It can be seen that this is the case if and only if the rank of \mathbf{P} equals m . A necessary condition for a well-defined MLS approximation is that at least m weight functions are non-zero (i.e. $n > m$) for each sample point $\mathbf{x} \in \Omega$ and that the nodes in Ω_s should not be arranged in a special pattern such as on a straight line. Here a sample point may be a nodal point under consideration or a quadrature point.

Solving for $\mathbf{a}(\mathbf{x})$ from Eq. (7) and substituting it into Eq. (5) yields a relation which may be written as the form of an interpolation function similar to that used in FEM, as

$$u^h(\mathbf{x}) = \Phi^T(\mathbf{x}) \cdot \hat{\mathbf{u}} = \sum_{i=1}^n \phi_i(\mathbf{x}) \hat{u}_i, \quad \mathbf{x} \in \Omega_s, \tag{10}$$

where $u^h(\mathbf{x}_i) \equiv u_i$ is not essentially equal to \hat{u}_i and,

$$\Phi^T(\mathbf{x}) = \mathbf{p}^T(\mathbf{x}) \mathbf{A}^{-1}(\mathbf{x}) \mathbf{B}(\mathbf{x}) \tag{11}$$

or

$$\phi_i(\mathbf{x}) = \sum_{j=1}^m p_j(\mathbf{x}) [\mathbf{A}^{-1}(\mathbf{x}) \mathbf{B}(\mathbf{x})]_{ji}. \tag{12}$$

Here, $\phi_i(\mathbf{x})$ is usually called the shape function of the MLS approximation corresponding to nodal point \mathbf{x}_i . From Eqs. (9) and (11), it is easily seen that $\phi_i(\mathbf{x}) = 0$ when $w_i(\mathbf{x}) = 0$. In practical applications, $w_i(\mathbf{x})$ is generally chosen such that it is non-zero over the support of nodal points \mathbf{x}_i . The support of the nodal points \mathbf{x}_i is usually taken to be a circle of radius r_s , centered at \mathbf{x}_i (see Fig. 1). The fact that $\phi_i(\mathbf{x}) = 0$, for \mathbf{x} not in the support of nodal point \mathbf{x}_i preserves the local character of the Moving Least Squares approximation.

Let $C^q(\Omega)$ be the space of q th continuously differentiable functions on Ω . If $w_i(\mathbf{x}) \in C^q(\Omega)$ and $p_j(\mathbf{x}) \in C^s(\Omega)$, $i = 1, 2, \dots, n$, $j = 1, 2, \dots, m$, then $\phi_i(\mathbf{x}) \in C^r(\Omega)$ with $r = \min(q, s)$. The partial derivatives of $\phi_i(\mathbf{x})$ are obtained as

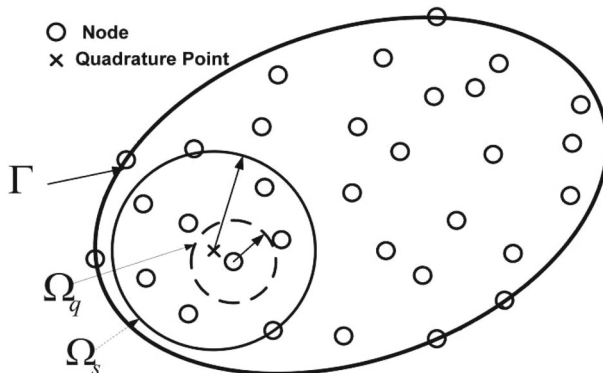


Fig. 1 Ω_s and Ω_q are local support and local quadrature domains, respectively

$$\phi_{i,k} = \sum_{j=1}^m [p_{j,k}(\mathbf{A}^{-1}\mathbf{B})_{ji} + p_j(\mathbf{A}^{-1}\mathbf{B}_{,k} + \mathbf{A}_{,k}^{-1}\mathbf{B})_{ji}] \tag{13}$$

in which $\mathbf{A}_{,k}^{-1} = (\mathbf{A}^{-1})_{,k}$ represents the derivative of the inverse of \mathbf{A} with respect to x^k , which is given by $\mathbf{A}_{,k}^{-1} = -\mathbf{A}^{-1}\mathbf{A}_{,k}\mathbf{A}^{-1}$, where $(\)_{,i}$ denotes $\partial(\)/\partial x_i$.

In this paper, the Gaussian weight function is applied as

$$w_i(\mathbf{x}) = \begin{cases} \frac{\exp\left[-\left(\frac{d_i}{c_i}\right)^2\right] - \exp\left[-\left(\frac{r_s}{c_i}\right)^2\right]}{1 - \exp\left[-\left(\frac{r_s}{c_i}\right)^2\right]}, & 0 \leq d_i \leq r_s, \\ 0, & d_i \geq r_s, \end{cases} \tag{14}$$

where $d_i = \|x - x_i\|$, c_i is a constant controlling the shape of the weight function w_i and r_s is the size of the support domain.

The size of support, r_s , of the weight function w_i associated with node i should be chosen such that r_s should be large enough to have sufficient number of nodes covered in the domain of definition of every sample point ($n \geq m$) to ensure the regularity of \mathbf{A} . A very small r_s may result in a relatively large numerical error in using Gauss numerical quadrature to calculate the entries in the system matrix. On the other hand, r_s should also be small enough to maintain the local character of the MLS approximation.

The Time Fractional Discretization of the Problem

According to Eq. (4), $\frac{\partial^\alpha u(\mathbf{x}, t)}{\partial t^\alpha}$ could be written as follows:

$$\frac{\partial^\alpha u(\mathbf{x}, t)}{\partial t^\alpha} = \begin{cases} \frac{1}{\Gamma(2-\alpha)} \int_0^t \frac{\partial^2 u(\mathbf{x}, \xi)}{\partial \xi^2} (t - \xi)^{1-\alpha} d\xi, & 1 < \alpha < 2, \\ \frac{\partial^2 u(\mathbf{x}, t)}{\partial t^2}, & \alpha = 2. \end{cases} \tag{15}$$

In order to discretize the problem in the time direction for $1 < \alpha < 2$, we substitute $t^{(n+1)}$ into Eq. (15), then the integral can be partitioned as

$$\begin{aligned} \frac{\partial^\alpha u(\mathbf{x}, t^{(n+1)})}{\partial t^\alpha} &= \frac{1}{\Gamma(2-\alpha)} \int_0^{t^{(n+1)}} \frac{\partial^2 u(\mathbf{x}, \xi)}{\partial \xi^2} (t^{(n+1)} - \xi)^{1-\alpha} d\xi \\ &= \frac{1}{\Gamma(2-\alpha)} \sum_{k=0}^n \int_{t^{(k)}}^{t^{(k+1)}} \frac{\partial^2 u(\mathbf{x}, \xi)}{\partial \xi^2} (t^{(n+1)} - \xi)^{1-\alpha} d\xi, \end{aligned} \tag{16}$$

where $t^{(0)} = 0$, $t^{(n+1)} = t^{(n)} + \Delta t$, $n = 0, 1, 2, \dots, M$, and $M\Delta t = T$. Approximations of the first and second order derivatives due to the finite difference formulae are defined as

$$\frac{\partial^2 u(\mathbf{x}, \sigma)}{\partial t^2} = \frac{u(\mathbf{x}, t^{(n+1)}) - 2u(\mathbf{x}, t^{(n)}) + u(\mathbf{x}, t^{(n-1)})}{\Delta t^2} + o(\Delta\sigma t + \Delta t^2), \tag{17}$$

$$\frac{\partial u(\mathbf{x}, t^{(n+1)})}{\partial t} = \frac{3u(\mathbf{x}, t^{(n+1)}) - 4u(\mathbf{x}, t^{(n)}) + u(\mathbf{x}, t^{(n-1)})}{2\Delta t} + o(\Delta t^2), \tag{18}$$

where $\sigma \in [t^{(n)}, t^{(n+1)}]$ and $\Delta_\sigma t = \sigma - t^{(n)}$. Replacing Eq. (17) into Eq. (16), gives

$$\begin{aligned} \frac{\partial^\alpha u(\mathbf{x}, t^{(n+1)})}{\partial t^\alpha} &= \frac{1}{\Gamma(2-\alpha)} \int_0^{t^{(n+1)}} \frac{\partial^2 u(\mathbf{x}, \xi)}{\partial \xi^2} (t^{(n+1)} - \xi)^{1-\alpha} d\xi \\ &\cong \frac{1}{\Gamma(2-\alpha)} \sum_{k=0}^n \frac{u^{(k+1)} - 2u^{(k)} + u^{(k-1)}}{\Delta t^2} \int_{t^{(k)}}^{t^{(k+1)}} (t^{(n+1)} - \xi)^{1-\alpha} d\xi, \end{aligned} \tag{19}$$

where $u^{(k)} = u(\mathbf{x}, t^{(k)})$, $k = 0, 1, 2, \dots, M$. In the above equation, the integral is easily obtained as

$$\int_{t^{(k)}}^{t^{(k+1)}} (t^{(n+1)} - \xi)^{1-\alpha} d\xi = \frac{1}{(2-\alpha)} \Delta t^{2-\alpha} [(n-k+1)^{2-\alpha} - (n-k)^{2-\alpha}]. \tag{20}$$

Rearrangement of Eqs. (19) and (18) by notation $b_k = (k+1)^{2-\alpha} - k^{2-\alpha}$ lead to

$$\begin{aligned} \frac{\partial^\alpha u(\mathbf{x}, t^{(n+1)})}{\partial t^\alpha} &= \frac{\Delta t^{-\alpha}}{\Gamma(3-\alpha)} \sum_{k=0}^n b_k [u^{(n-k+1)} - 2u^{(n-k)} + u^{(n-k-1)}] \\ &\cong a_0 \left\{ u^{(n+1)} - 2u^{(n)} + u^{(n-1)} + \sum_{k=1}^n b_k [u^{(n-k+1)} - 2u^{(n-k)} + u^{(n-k-1)}] \right\}, \end{aligned} \tag{21}$$

and

$$\frac{\partial u(\mathbf{x}, t^{(n+1)})}{\partial t} \cong a'_0 (3u^{(n+1)} - 4u^{(n)} + u^{(n-1)}), \tag{22}$$

where $a_0 = \frac{\Delta t^{-\alpha}}{\Gamma(3-\alpha)}$, $a'_0 = \frac{1}{2\Delta t}$ and $n = 0, 1, 2, \dots, M$. We note that Eq. (1) at $t = t^{(n+1)}$ due to θ -weighted finite difference formulation is as follows:

$$\frac{\partial^\alpha u(\mathbf{x}, t^{(n+1)})}{\partial t^\alpha} + \gamma_1 \frac{\partial u(\mathbf{x}, t^{(n+1)})}{\partial t} = \gamma_2 [\theta \Delta u^{(n+1)} + (1-\theta) \Delta u^{(n)}] + f^{(n+1)}, \tag{23}$$

where, $0 < \theta < 1$ is a constant, $\Delta u^{(n)} = \Delta u(\mathbf{x}, t^{(n)})$ and $f^{(n)} = f(\mathbf{x}, t^{(n)})$. We set $\theta = \frac{1}{2}$ for simplicity, and substitute Eqs. (21) and (22) into Eq. (23), then we obtain

$$\begin{aligned} &a_0 \left\{ u^{(n+1)} - 2u^{(n)} + u^{(n-1)} + \sum_{k=1}^n b_k [u^{(n-k+1)} - 2u^{(n-k)} + u^{(n-k-1)}] \right\} \\ &+ \gamma_1 a'_0 (3u^{(n+1)} - 4u^{(n)} + u^{(n-1)}) = \frac{1}{2} \gamma_2 [\Delta u^{(n+1)} + \Delta u^{(n)}] + f^{(n+1)}, \end{aligned}$$

or equivalently

$$\begin{aligned} \frac{1}{2} \gamma_2 \Delta u^{(n+1)} - (a_0 + 3\gamma_1 a'_0) u^{(n+1)} &= -\frac{1}{2} \gamma_2 \Delta u^{(n)} - (2a_0 + 4\gamma_1 a'_0) u^{(n)} \\ &+ \sum_{k=1}^n a_0 b_k [u^{(n-k+1)} - 2u^{(n-k)} + u^{(n-k-1)}] \\ &+ (a_0 + \gamma_1 a'_0) u^{(n-1)} - f^{(n+1)}. \end{aligned} \tag{24}$$

The Local Weak Form of the MLPG

Instead of giving the global weak form, the meshless local Galerkin weak form method constructs the weak form over local quadrature cell such as Ω_q , which is a small region taken for each node in the global domain Ω (see Fig. 1). The local quadrature cells overlap each other and cover the whole global domain Ω . The local quadrature cells could be of any geometric shape and size. In this paper they are taken to be of circular shape. The local weak form of Eq. (24) for $\mathbf{x}_i = (x_i, y_i) \in \Omega_q^i$ can be written as

$$\begin{aligned} & \int_{\Omega_q^i} \left[\frac{1}{2} \gamma_2 \Delta u^{(n+1)} - (a_0 + 3\gamma_1 a'_0) u^{(n+1)} \right] v(\mathbf{x}) d\Omega \\ &= \int_{\Omega_q^i} \left[-\frac{1}{2} \gamma_2 \Delta u^{(n)} - (2a_0 + 4\gamma_1 a'_0) u^{(n)} + (a_0 + \gamma_1 a'_0) u^{(n-1)} \right] v(\mathbf{x}) d\Omega \\ &+ \int_{\Omega_q^i} \left(\sum_{k=1}^n a_0 b_k [u^{(n-k+1)} - 2u^{(n-k)} + u^{(n-k-1)}] \right) v(\mathbf{x}) d\Omega - \int_{\Omega_q^i} f^{(n+1)} v(\mathbf{x}) d\Omega, \end{aligned} \tag{25}$$

where Ω_q^i is the local quadrature domain associated with the point i , i.e., it is a circle centered at \mathbf{x}_i of radius r_q and, $v(\mathbf{x})$ is the Heaviside step function [47, 48],

$$v(\mathbf{x}) = \begin{cases} 1, & \mathbf{x} \in \Omega_q, \\ 0, & \mathbf{x} \notin \Omega_q, \end{cases} \tag{26}$$

as the test function in each local quadrature domain. Using the divergence theorem, Eq. (25) yields the following expression:

$$\begin{aligned} & -(a_0 + 3\gamma_1 a'_0) \int_{\Omega_q^i} u^{(n+1)} v(\mathbf{x}) d\Omega - \frac{1}{2} \gamma_2 \int_{\Omega_q^i} \nabla u^{(n+1)} \nabla v d\Omega + \frac{1}{2} \gamma_2 \int_{\partial\Omega_q^i} v \frac{\partial u^{(n+1)}}{\partial n} d\Gamma \\ &= \frac{1}{2} \gamma_2 \int_{\Omega_q^i} \nabla u^{(n)} \nabla v d\Omega - \frac{1}{2} \gamma_2 \int_{\partial\Omega_q^i} v \frac{\partial u^{(n)}}{\partial n} d\Gamma - (2a_0 + 4\gamma_1 a'_0) \int_{\Omega_q^i} u^{(n)} v(\mathbf{x}) d\Omega \\ &+ \sum_{k=1}^n a_0 b_k \left[\int_{\Omega_q^i} u^{(n-k+1)} v(\mathbf{x}) d\Omega - 2 \int_{\Omega_q^i} u^{(n-k)} v(\mathbf{x}) d\Omega + \int_{\Omega_q^i} u^{(n-k-1)} v(\mathbf{x}) d\Omega \right] \\ &+ (a_0 + \gamma_1 a'_0) \int_{\Omega_q^i} u^{(n-1)} v(\mathbf{x}) d\Omega - \int_{\Omega_q^i} f^{(n+1)} v(\mathbf{x}) d\Omega, \end{aligned} \tag{27}$$

where $\partial\Omega_q^i$ is the boundary of Ω_q^i , $n = (n_1, n_2)$ is the outward unit normal to the boundary $\partial\Omega_q^i$, and

$$\frac{\partial u}{\partial n} = \frac{\partial u}{\partial x} n_1 + \frac{\partial u}{\partial y} n_2$$

is the normal derivative, i.e., the derivative in the outward normal direction to the boundary $\partial\Omega_q^i$. Because the derivative of the Heaviside step function $v(\mathbf{x})$ is equal to zero, then the local weak form Eq. (27) is changed into the following simple integral equation:

$$\begin{aligned} & -(a_0 + 3\gamma_1 a'_0) \int_{\Omega_q^i} u^{(n+1)} d\Omega + \frac{1}{2} \gamma_2 \int_{\partial\Omega_q^i} \frac{\partial u^{(n+1)}}{\partial n} d\Gamma = -\frac{1}{2} \gamma_2 \int_{\partial\Omega_q^i} \frac{\partial u^{(n)}}{\partial n} d\Gamma \\ & - (2a_0 + 4\gamma_1 a'_0) \int_{\Omega_q^i} u^{(n)} d\Omega + (a_0 + \gamma_1 a'_0) \int_{\Omega_q^i} u^{(n-1)} d\Omega \end{aligned}$$

$$\begin{aligned}
 & + \sum_{k=1}^n a_0 b_k \left[\int_{\Omega_q^i} u^{(n-k+1)} d\Omega - 2 \int_{\Omega_q^i} u^{(n-k)} d\Omega + \int_{\Omega_q^i} u^{(n-k-1)} d\Omega \right] \\
 & - \int_{\Omega_q^i} f^{(n+1)} d\Omega.
 \end{aligned} \tag{28}$$

Applying the moving least squares (MLS) approximation for the unknown functions, the local integral Eq. (28) is transformed into a system of algebraic equations with used unknown quantities, as described in the next section.

Numerical Implementation of MLPG: Reducing to Linear Algebraic System

In this section, we consider Eq. (28) to see how to obtain discrete equations. Consider N regularly located points on the boundary and the domain of the problem (i.e. $\Omega \subseteq \mathbb{R}^2$) so that the distance between to consecutive nodes in each direction is constant and equal to h . Assuming that $u(\mathbf{x}_i, k\Delta t)$ for all $k = 1, 2, \dots, n$ and $i = 1, 2, \dots, N$ are known, our aim is to compute $u(\mathbf{x}_i, (n + 1)\Delta t)$, $i = 1, 2, \dots, N$. So, we have N unknowns and to compute these unknowns we need N equations. As it will be described, corresponding to each node we obtain one equation. For nodes which are located in the interior of the domain, i.e., for $\mathbf{x}_i \in$ interior Ω , to obtain the discrete equations from the locally weak forms (28), substituting approximation formula (10) into local integral equations (28) yields:

$$\begin{aligned}
 & -(a_0 + 3\gamma_1 a'_0) \sum_{j=1}^N \left(\int_{\Omega_q^i} \phi_j d\Omega \right) u_j^{(n+1)} + \frac{1}{2} \gamma_2 \sum_{j=1}^N \left(\int_{\partial\Omega_q^i} \frac{\partial \phi_j}{\partial n} d\Gamma \right) u_j^{(n+1)} \\
 & = -\frac{1}{2} \gamma_2 \sum_{j=1}^N \left(\int_{\partial\Omega_q^i} \frac{\partial \phi_j}{\partial n} d\Gamma \right) u_j^{(n)} - (2a_0 + 4\gamma_1 a'_0) \sum_{j=1}^N \left(\int_{\Omega_q^i} \phi_j d\Omega \right) u_j^{(n)} \\
 & + \sum_{k=1}^n a_0 b_k \left[\sum_{j=1}^N \left(\int_{\Omega_q^i} \phi_j d\Omega \right) u_j^{(n-k+1)} \right. \\
 & \quad \left. - 2 \sum_{j=1}^N \left(\int_{\Omega_q^i} \phi_j d\Omega \right) u_j^{(n-k)} + \sum_{j=1}^N \left(\int_{\Omega_q^i} \phi_j d\Omega \right) u_j^{(n-k-1)} \right] \\
 & + (a_0 + \gamma_1 a'_0) \sum_{j=1}^N \left(\int_{\Omega_q^i} \phi_j d\Omega \right) u_j^{(n-1)} - \int_{\Omega_q^i} f^{(n+1)} d\Omega.
 \end{aligned} \tag{29}$$

We had supposed $b_k = (k + 1)^{2-\alpha} - (k)^{2-\alpha}$, $k = 1, 2, \dots, n$ in the section 3, in addition assume $b_{-1} = 0$ and $b_0 = 1$. By these assumptions Eq. (29) is converted to the following equation

$$\begin{aligned}
 & \left[-(a_0 + 3\gamma_1 a'_0) \sum_{j=1}^N \left(\int_{\Omega_q^i} \phi_j d\Omega \right) + \frac{1}{2} \gamma_2 \sum_{j=1}^N \left(\int_{\partial\Omega_q^i} \frac{\partial \phi_j}{\partial n} d\Gamma \right) \right] u_j^{(n+1)} \\
 & = \sum_{s=1}^n \left\{ [a_0(b_{n-s-1} - 2b_{n-s} + b_{n-s+1})] \sum_{j=1}^N \left(\int_{\Omega_q^i} \phi_j d\Omega \right) u_j^{(s)} \right\}
 \end{aligned}$$

$$\begin{aligned}
 & -4\gamma_1 a'_0 \sum_{j=1}^N \left(\int_{\Omega_q^i} \phi_j d\Omega \right) u_j^{(n)} \\
 & -2a_0 b_n \sum_{j=1}^N \left(\int_{\Omega_q^i} \phi_j d\Omega \right) u_j^{(0)} + a_0 b_n \sum_{j=1}^N \left(\int_{\Omega_q^i} \phi_j d\Omega \right) u_j^{(-1)} \\
 & -\frac{1}{2} \gamma_2 \sum_{j=1}^N \left(\int_{\partial\Omega_q^i} \frac{\partial \phi_j}{\partial n} d\Gamma \right) u_j^{(n)} + \gamma_1 a'_0 \sum_{j=1}^N \left(\int_{\Omega_q^i} \phi_j d\Omega \right) u_j^{(n-1)} - \int_{\Omega_q^i} f^{(n+1)} d\Omega.
 \end{aligned} \tag{30}$$

According to the initial conditions that were introduced in Eq. (2), we apply the following assumptions:

$$u_j^{(0)} = \varphi(\mathbf{x}_j), \quad u_j^{(-1)} = u_j^{(1)} - 2\Delta t \psi(\mathbf{x}_j), \tag{31}$$

where, the second relation is the result of central finite difference formula, then we conclude the following

$$\sum_{j=1}^N \left(\int_{\Omega_q^i} \phi_j d\Omega \right) u_j^{(0)} = \int_{\Omega_q^i} \varphi(\mathbf{x}) d\Omega, \tag{32}$$

$$\sum_{j=1}^N \left(\int_{\Omega_q^i} \phi_j d\Omega \right) u_j^{(-1)} = \sum_{j=1}^N \left(\int_{\Omega_q^i} \phi_j d\Omega \right) u_j^{(1)} - 2\Delta t \int_{\Omega_q^i} \psi(\mathbf{x}) d\Omega. \tag{33}$$

Therefore, applying Eqs. (32) and (33) into (30) yields

$$\begin{aligned}
 & \left[-(a_0 + 3\gamma_1 a'_0) \sum_{j=1}^N \left(\int_{\Omega_q^i} \phi_j d\Omega \right) + \frac{1}{2} \gamma_2 \sum_{j=1}^N \left(\int_{\partial\Omega_q^i} \frac{\partial \phi_j}{\partial n} d\Gamma \right) \right] u_j^{(n+1)} \\
 & = \sum_{s=1}^n \left\{ [a_0(b_{n-s-1} - 2b_{n-s} + b_{n-s+1})] \sum_{j=1}^N \left(\int_{\Omega_q^i} \phi_j d\Omega \right) u_j^{(s)} \right\} \\
 & - 4\gamma_1 a'_0 \sum_{j=1}^N \left(\int_{\Omega_q^i} \phi_j d\Omega \right) u_j^{(n)} \\
 & + a_0 b_n \sum_{j=1}^N \left(\int_{\Omega_q^i} \phi_j d\Omega \right) u_j^{(1)} - \frac{1}{2} \gamma_2 \sum_{j=1}^N \left(\int_{\partial\Omega_q^i} \frac{\partial \phi_j}{\partial n} d\Gamma \right) u_j^{(n)} \\
 & + \gamma_1 a'_0 \sum_{j=1}^N \left(\int_{\Omega_q^i} \phi_j d\Omega \right) u_j^{(n-1)} \\
 & - \int_{\Omega_q^i} f^{(n+1)} d\Omega - 2a_0 b_n \int_{\Omega_q^i} \varphi(\mathbf{x}) d\Omega - 2a_0 b_n \Delta t \int_{\Omega_q^i} \psi(\mathbf{x}) d\Omega.
 \end{aligned} \tag{34}$$

For nodes which are located on the boundary, we set

$$u^{(n+1)}(\mathbf{x}_i) = g(\mathbf{x}_i, (n + 1)\Delta t), \quad \mathbf{x}_i \in \Gamma. \tag{35}$$

The matrix forms of Eqs. (34)–(35) for all N nodal points in the domain and the boundary of the problem are given below:

$$\begin{aligned} & \left[-(a_0 + 3\gamma_1 a'_0) \sum_{j=1}^N A_{ij} + \frac{1}{2} \gamma_2 \sum_{j=1}^N B_{ij} \right] u_j^{(n+1)} = -4\gamma_1 a'_0 \sum_{j=1}^N A_{ij} u_j^{(n)} \\ & \sum_{s=1}^n \left\{ [a_0(b_{n-s-1} - 2b_{n-s} + b_{n-s+1})] \sum_{j=1}^N A_{ij} u_j^{(s)} \right\} + a_0 b_n \sum_{j=1}^N A_{ij} u_j^{(1)} \\ & + \gamma_1 a'_0 \sum_{j=1}^N A_{ij} u_j^{(n-1)} - \frac{1}{2} \gamma_2 \sum_{j=1}^N B_{ij} u_j^{(n)} - F_i^{(n+1)} - 2a_0 b_n \Phi_i - 2a_0 b_n \Delta t \Psi_i, \end{aligned} \tag{36}$$

where

$$A_{ij} = \int_{\Omega_q^i} \phi_j d\Omega, \quad B_{ij} = \int_{\partial\Omega_q^i} \frac{\partial \phi_j}{\partial n} d\Gamma, \quad F_i^{(n+1)} = \int_{\Omega_q^i} F(\mathbf{x}, (n+1)\Delta t) d\Omega, \tag{37}$$

$$\Phi_i = \int_{\Omega_q^i} \varphi(\mathbf{x}) d\Omega, \quad \Psi_i = \int_{\Omega_q^i} \psi(\mathbf{x}) d\Omega. \tag{38}$$

By considering the following notations

$$\begin{aligned} \mathbf{A}_{ij} &= -(a_0 + 3\gamma_1 a'_0) \sum_{j=1}^N A_{ij} + \frac{1}{2} \gamma_2 \sum_{j=1}^N B_{ij}, \\ \alpha_{n,s} &= a_0(b_{n-s-1} - 2b_{n-s} + b_{n-s+1}), \\ \beta_n &= a_0 b_n, \\ \lambda_1 &= -\frac{1}{2} \gamma_2, \\ \lambda_2 &= -\gamma_1 a'_0, \\ \delta_n &= -2a_0 b_n, \\ \mu_n &= -2a_0 b_n \Delta t, \\ \mathbf{F}^{n+1} &= [F_1^{(n+1)}, F_2^{(n+1)}, \dots, F_N^{(n+1)}]^T, \\ \Phi &= [\Phi_1, \Phi_2, \dots, \Phi_N]^T, \\ \Psi &= [\Psi_1, \Psi_2, \dots, \Psi_N]^T, \\ \mathbf{U}^{n+1} &= [u_1^{(n+1)}, u_2^{(n+1)}, \dots, u_N^{(n+1)}]^T, \end{aligned}$$

Equation (36) changes to the following matrix form

$$\begin{aligned} \mathbf{A} \mathbf{U}^{(n+1)} &= [\lambda_1 B + 4\lambda_2 A] \mathbf{U}^{(n)} - \lambda_2 A \mathbf{U}^{(n-1)} + \sum_{s=1}^n \left\{ \alpha_{n,s} A \mathbf{U}^{(s)} \right\} \\ &+ \beta_n A \mathbf{U}^{(1)} + \delta_n \Phi + \mu_n \Psi - \mathbf{F}^{n+1}. \end{aligned} \tag{39}$$

Furthermore, to satisfy Eq. (35), for all nodes belong to the boundary, i.e. $\mathbf{x}_i \in \Gamma$, we set

$$\Phi_i = \Psi_i = 0, \quad \forall j : A_{ij} = B_{ij} = 0, \quad \mathbf{F}_i^{(n+1)} = -g(\mathbf{x}_i, (n+1)\Delta t), \quad \mathbf{A}_{ij} = \begin{cases} 1, & j = i \\ 0, & j \neq i \end{cases} \tag{40}$$

for each step. We notice here that, when $n = 0$, we use directly (29) and then for $n > 0$ it is straightforward to use Eq. (39).

Error Analysis

Given positive N , let $\tau = T/N$, $t_n = n\tau$ ($0 \leq n \leq N$). The time domain $[0, T]$ is covered by $\{t_n | 0 \leq n \leq N\}$. Given grid function $v = \{v^n | 0 \leq n \leq N\}$, we denote:

$$v^{n-1/2} = \frac{1}{2}(v^n + v^{n-1}), \quad \partial_t v^{n-1/2} = \frac{v^n - v^{n-1}}{\tau} \tag{41}$$

Lemma 1 Suppose $1 < \alpha < 2$, $\in C^2[0, T]$. It holds

$$\begin{aligned} & \left| \frac{1}{\Gamma(2-\alpha)} \int_0^{t_n} \frac{\mathcal{G}'(\xi)}{(t_n-\xi)^{\alpha-1}} d\xi \right. \\ & \quad \left. - \frac{\tau^{1-\alpha}}{\Gamma(3-\alpha)} \left[a_0 \mathcal{G}(t_n) - \sum_{k=1}^{n-1} (a_{n-k-1} - a_{n-k}) \mathcal{G}(t_k) - a_{n-1} \mathcal{G}(0) \right] \right| \\ & \leq \frac{1}{\Gamma(3-\alpha)} \left[\frac{2-\alpha}{12} + \frac{2^{3-\alpha}}{3-\alpha} - (1+2^{1-\alpha}) \right] \max_{0 \leq t \leq t_n} |\mathcal{G}''(t)| \tau^{3-\alpha} \end{aligned} \tag{42}$$

where

$$a_k = (k+1)^{2-\alpha} - k^{2-\alpha}. \tag{43}$$

Proof See [35] for more details.

Theorem 1 The scheme (24) is unconditionally stable in the sense that for all $\tau > 0$, it holds

$$\|U^n\|^2 \leq C \left(\|\nabla U^0\|^2 + \frac{t_n^{2-\alpha}}{\Gamma(3-\alpha)} \|U_t^0\|^2 + 2 \frac{t_n}{\gamma_1} \max_{1 \leq k \leq n} \|f^{k-1/2}\|^2 \right). \tag{44}$$

Proof Choosing $v = \partial_t U^{n-1/2}$ in (42) and noticing $a_0 = 1$ and $\mu_1 = \Gamma(3-\alpha)\tau^{\alpha-1}$ then we have the following equation for $1 \leq n \leq N$:

$$\begin{aligned} & \frac{1}{\mu_1} \|\partial_t U^{n-1/2}\|^2 + (\nabla U^{n-1/2}, \nabla \partial_t U^{n-1/2}) + \gamma_1 (\partial_t U^{n-1/2}, \partial_t U^{n-1/2}) \\ & = \frac{1}{\mu_1} \left[\sum_{k=1}^{n-1} (a_{n-k-1} - a_{n-k}) (\partial_t U_t^{k-1/2}, \partial_t U^{n-1/2}) - a_{n-1} (U_t^0, \partial_t U^{n-1/2}) \right] \\ & \quad + (f^{n-1/2}, \partial_t U^{n-1/2}), \quad 1 \leq n \leq N, \end{aligned} \tag{45}$$

Since

$$\begin{aligned} (\nabla U^{n-1/2}, \nabla \partial_t U^{n-1/2}) & = \left(\frac{\nabla U^n - \nabla U^{n-1}}{2}, \frac{\nabla U^n + \nabla U^{n-1}}{\tau} \right) \\ & = \frac{1}{2\tau} (\|\nabla U^n\|^2 - \|\nabla U^{n-1}\|^2). \end{aligned} \tag{46}$$

and noticing a_{k-1} and $(a_{n-k-1} - a_{n-k})$ are positive, hence

$$\begin{aligned} & \frac{1}{\mu_1} \|\partial_t \mathcal{U}^{n-1/2}\|^2 + \frac{1}{2\tau} (\|\nabla \mathcal{U}^n\|^2 - \|\nabla \mathcal{U}^{n-1}\|^2) + \gamma_1 (\partial_t \mathcal{U}^{n-1/2}, \partial_t \mathcal{U}^{n-1/2}) \\ &= \frac{1}{\mu_1} \left[\sum_{k=1}^{n-1} (a_{n-k-1} - a_{n-k}) |(\partial_t \mathcal{U}^{k-1/2}, \partial_t \mathcal{U}^{n-1/2})| - a_{n-1} |U_t^0, \partial_t \mathcal{U}^{n-1/2}| \right] \\ & \quad + |(f^{n-1/2}, \partial_t \mathcal{U}^{n-1/2})|, \quad 1 \leq n \leq N, \end{aligned} \tag{47}$$

Then we can rewrite:

$$\begin{aligned} & \frac{2\tau}{\mu_1} \|\partial_t \mathcal{U}^{n-1/2}\|^2 + (\|\nabla \mathcal{U}^n\|^2 - \|\nabla \mathcal{U}^{n-1}\|^2) + 2\gamma_1 \tau \|\partial_t \mathcal{U}^{n-1/2}\|^2 \\ & \leq \frac{\tau}{\mu_1} \left[\sum_{k=1}^{n-1} (a_{n-k-1} - a_{n-k}) (\|\partial_t \mathcal{U}^{k-1/2}\|^2 + \|\partial_t \mathcal{U}^{n-1/2}\|^2) - a_{n-1} (\|U_t^0\|^2 + \|\partial_t \mathcal{U}^{n-1/2}\|^2) \right] \\ & \quad + 2\tau |(f^{n-1/2}, \partial_t \mathcal{U}^{n-1/2})|, \quad 1 \leq n \leq N. \end{aligned} \tag{48}$$

On the other hand

$$\begin{aligned} & \frac{\tau}{\mu_1} \|\partial_t \mathcal{U}^{n-1/2}\|^2 + \|\nabla \mathcal{U}^n\|^2 - \|\nabla \mathcal{U}^{n-1}\|^2 + 2\gamma_1 \tau \|\mathcal{U}^{n-1/2}\|^2 \\ &= \frac{\tau}{\mu_1} \left[\sum_{k=1}^{n-1} (a_{n-k-1} - a_{n-k}) \|\partial_t \mathcal{U}^{k-1/2}\|^2 - a_{n-1} \|U_t^0\|^2 \right] \\ & \quad + 2\tau |(f^{n-1/2}, \partial_t \mathcal{U}^{n-1/2})|, \quad 1 \leq n \leq N. \end{aligned} \tag{49}$$

We may consider without loss of generality $0 < 2\gamma_1 \tau < 1$, then we obtain

$$\begin{aligned} & \frac{\tau}{\mu_1} \sum_{k=1}^n a_{n-k} \|\partial_t \mathcal{U}^{k-1/2}\|^2 + \|\nabla \mathcal{U}^n\|^2 \\ &= \frac{\tau}{\mu_1} \sum_{k=1}^{n-1} a_{n-k-1} \|\partial_t \mathcal{U}^{k-1/2}\|^2 + \|\nabla \mathcal{U}^{n-1}\|^2 - a_{n-1} \|U_t^0\|^2 + \tau \frac{\|f^{n-1/2}\|}{2\gamma_1}, \quad 1 \leq n \leq N, \end{aligned}$$

where

$$2\tau |(f^{n-1/2}, \partial_t \mathcal{U}^{n-1/2})| \leq 2\tau \frac{\|f^{n-1/2}\|^2}{\gamma_1} + 2\gamma_1 \tau \|\partial_t \mathcal{U}^{n-1/2}\|^2. \tag{50}$$

Denoting

$$\mathbb{E}^n = \|\nabla \mathcal{U}^n\|^2 + \frac{\tau}{\mu_1} \sum_{k=1}^n a_{n-k} \|\partial_t \mathcal{U}^{k-1/2}\|^2, \quad n \geq 1, \tag{51}$$

consequently, we reach to the following inequality

$$\begin{aligned} \mathbb{E}^n & \leq \mathbb{E}^{n-1} + \frac{\tau a_{n-1}}{\mu_1} \|U_t^0\|^2 + \frac{2\tau}{\gamma_1} \|f^{n-1/2}\|^2 \\ & \leq \mathbb{E}^0 + \frac{\tau}{\mu_1} \sum_{k=1}^n a_{k-1} \|U_t^0\|^2 + \frac{2\tau}{\gamma_1} \sum_{k=1}^n \|f^{k-1/2}\|^2 \\ & \leq \mathbb{E}^0 + \frac{\tau}{\mu_1} \sum_{k=1}^n a_{k-1} \|U_t^0\|^2 + \frac{2\tau n}{\gamma_1} \max_{1 \leq k \leq n} \|f^{k-1/2}\|^2 \end{aligned}$$

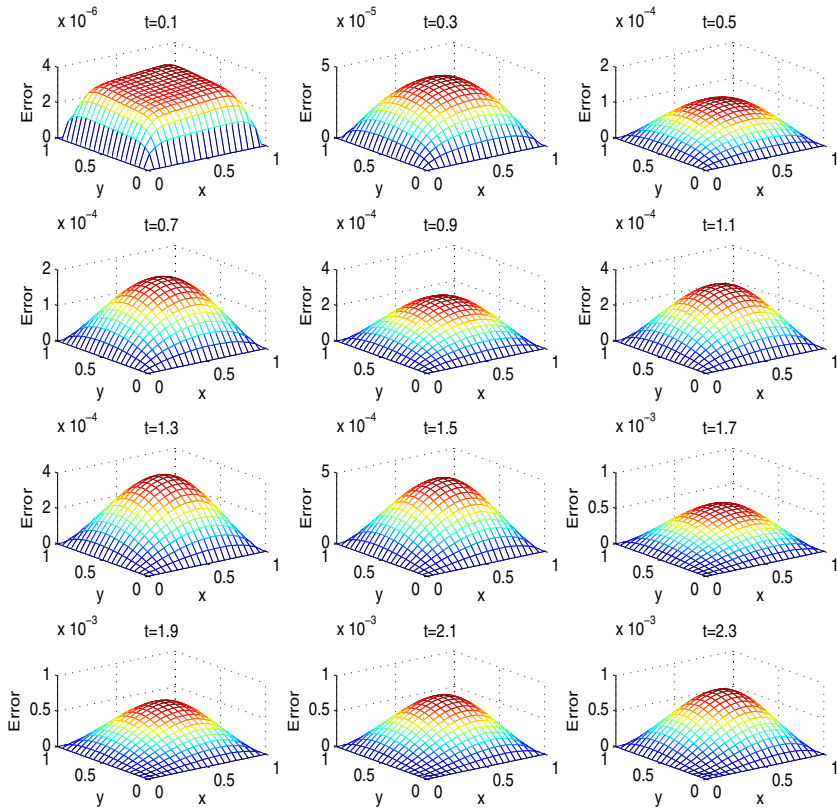


Fig. 2 Absolute error of MLPG solutions with $\Delta t = 0.001$, $N = 441$ and $\alpha = \frac{3}{2}$ for Example 1

It is easy to verify that $\sum_{k=1}^n a_{k-1} = n^{2-\alpha}$, therefore, we have

$$\frac{\tau}{\Gamma(1)} \sum_{k=1}^n a_{k-1} \|U_t^0\|^2 = \frac{t_n^{2-\alpha}}{\Gamma(3-\alpha)} \|U_t^0\|^2. \tag{52}$$

It could be rewritten

$$\|U^n\|^2 \leq C \left(\|\nabla U^0\|^2 + \frac{\tau}{\Gamma(1)} \sum_{k=1}^n a_{k-1} \|U_t^0\|^2 + 2 \frac{n\tau}{\gamma_1} \max_{1 \leq k \leq n} \|f^{k-1/2}\|^2 \right) \tag{53}$$

Hence the proof is complete. □

Two Numerical Experiments

In this section, we show the results obtained for two examples using the meshless method described above. In both examples, the domain integrals are evaluated with 16 points Gaussian quadrature rule while the boundary integrals are evaluated with 7 points Gaussian quadrature rule. To show the behavior of the solution and the efficiency of the proposed method, the following absolute error is applied to make comparison

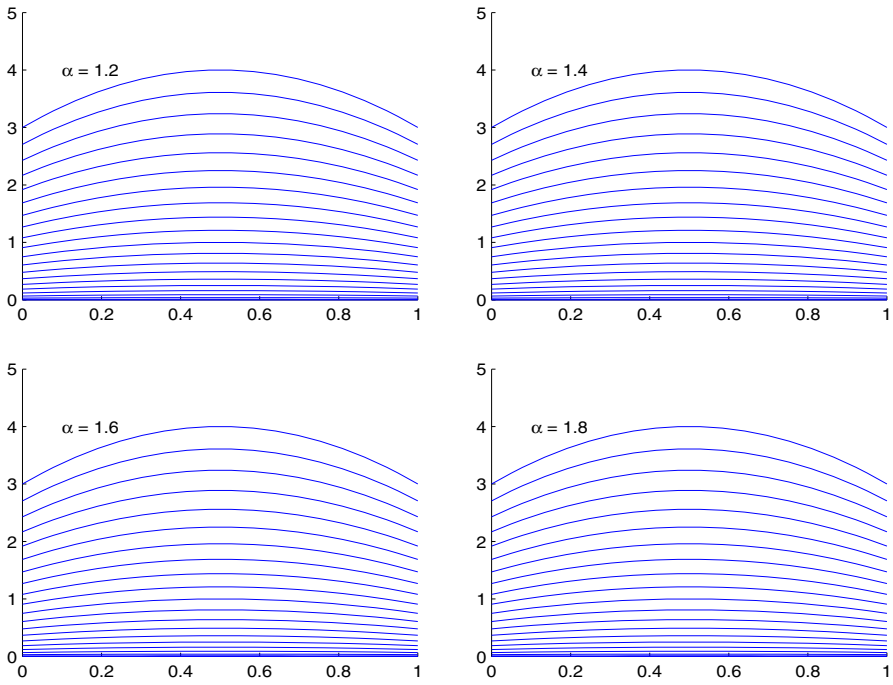


Fig. 3 Diagram of MLPG solutions $u(x, 0.5, t)$ at $t = 0, 0.1, 0.2, \dots, 2$ with $\Delta t = 0.001$ and $N = 441$ for Example 1

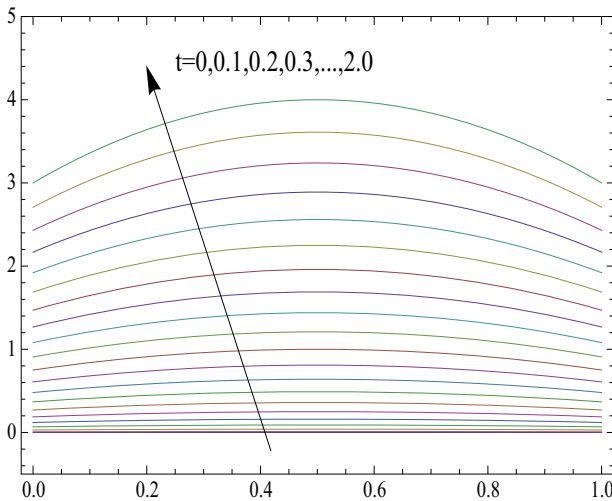


Fig. 4 Diagram of exact solutions $u(x, 0.5, t)$ at $t = 0, 0.1, 0.2, \dots, 2$ for Example 1

$$Error = \max_{1 \leq i \leq N} |U_{exact}(\mathbf{x}_i) - U_{approx}(\mathbf{x}_i)|$$

where $U_{exact}(\mathbf{x}_i)$ and $U_{approx}(\mathbf{x}_i)$ are achieved by exact and approximate solution and N is number of nodal points. In both problems the regular node distribution is used. Also in

Table 1 The L_∞ error with fixed $N = 441$, $\alpha = 1.5$ and different time-steps for Example 1

t	$\Delta t = 0.1$	$\Delta t = 0.01$	$\Delta t = 0.001$
$t = 0.000000$	0.00000000	0.00000000	0.00000000
$t = 0.100000$	0.00021788	0.00003173	0.00000349
$t = 0.200000$	0.00139839	0.00016792	0.00001750
$t = 0.300000$	0.00364989	0.00041713	0.00004267
$t = 0.400000$	0.00673507	0.00073569	0.00007486
$t = 0.500000$	0.01024647	0.00108049	0.00010982
$t = 0.600000$	0.01384541	0.00142623	0.00014512
$t = 0.700000$	0.01735184	0.00176128	0.00017966
$t = 0.800000$	0.02070118	0.00208286	0.00021318
$t = 0.900000$	0.02389343	0.00239296	0.00024589
$t = 1.000000$	0.02696163	0.00269532	0.00027814

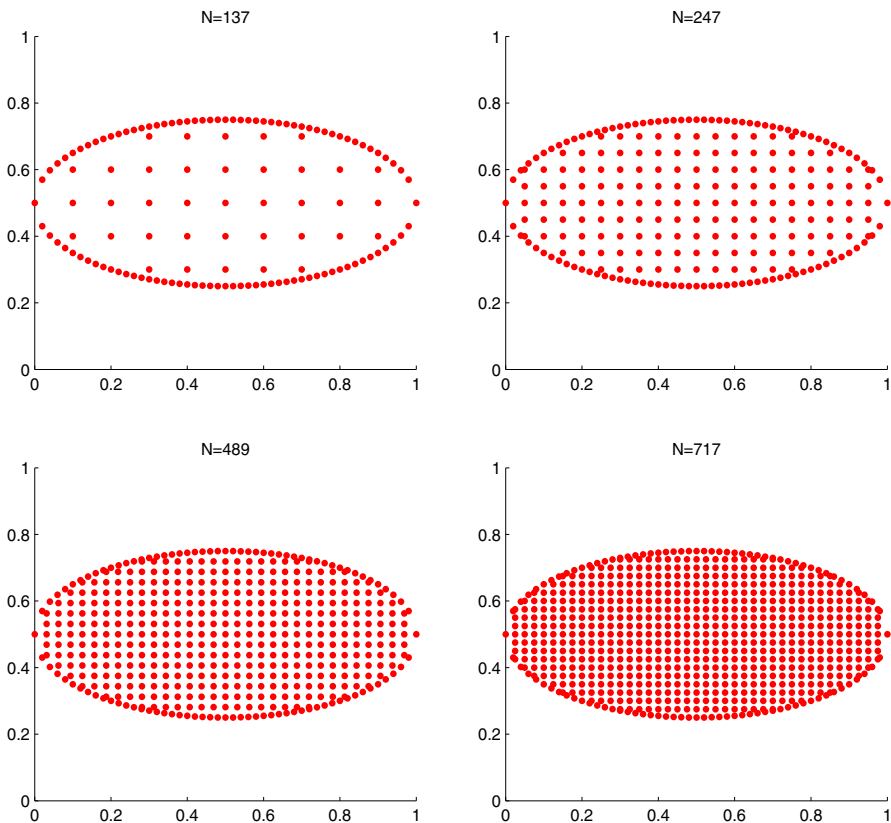


Fig. 5 The approximation of the domain of Example 2 by different number of nodal points

order to implement the meshless local weak form, the radius of the local quadrature domain $r_q = 0.7h$ is selected, where h is the distance between the nodes in x or y direction. The size of r_q is such that the union of these sub-domains must cover the whole global domain.

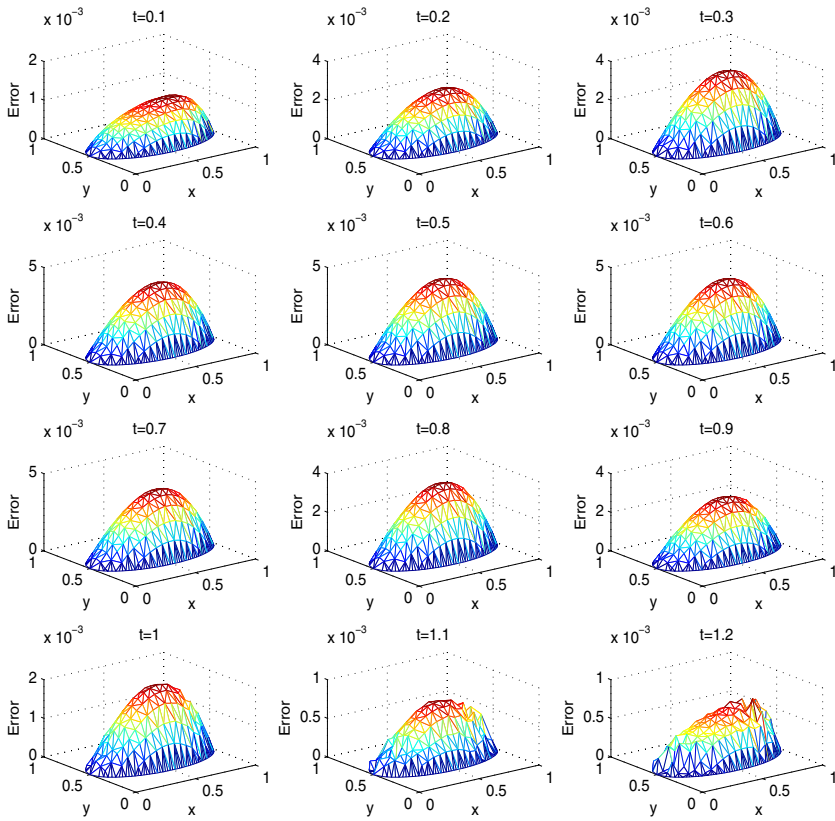


Fig. 6 Absolute error of MLPG solutions with $\Delta t = 0.05$, $N = 247$ and $\alpha = 1.2$ for Example 2

The radius of support domain to moving least squares approximation is $r_s = 4r_q$ and all shape parameters in (14) are chosen $c_i = c = 1.2h$. This size is significant enough to have sufficient number of nodes (n) and gives an appropriate shape functions. Also, the quadratic basis functions is used i.e. $m = 6$ is taken.

Example 1 (Regular domain) We set $\gamma_1 = \gamma_2 = 1$, the exact solution of problem (1)–(3) is taken as

$$u(x, y, t) = t^2(2 - x - y)(x + y),$$

and the domain of the problem is $\Omega = [0, 1] \times [0, 1]$. The functions $\varphi(x, y)$, $\psi(x, y)$ and $g(x, y, t)$ are defined accordingly, and also $f(x, y, t)$ is given by

$$f(x, y, t) = \frac{2t^{2-\alpha}(x + y - 2)(x + y)}{(\alpha - 2)\Gamma(2 - \alpha)} + 4t^2 + 2t(-x - y + 2)(x + y),$$

where

$$\Gamma(z) = \int_0^\infty t^{z-1} \exp(-t) dt. \tag{54}$$

Figure 2 presents the absolute error of approximate MLPG solutions at different time levels with $\Delta t = 0.001$ and $N = 441(h = 0.05)$ for $\alpha = 1.5$. Also, the approximate MLPG

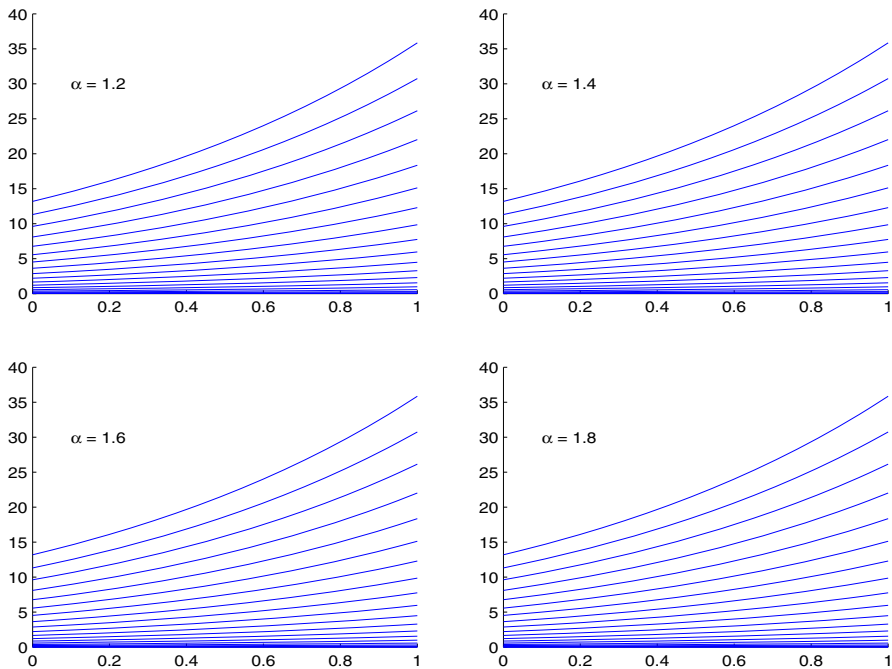
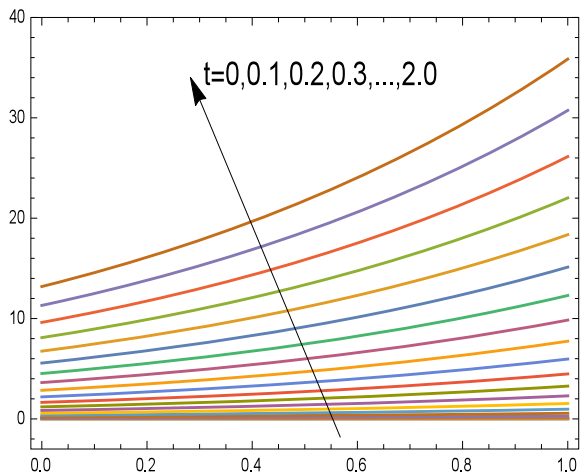


Fig. 7 Diagram of MLPG solutions $u(x, 0.5, t)$ at $t = 0, 0.1, 0.2, \dots, 2$ with $\Delta t = 0.05$ and $N = 247$ for Example 2

Fig. 8 Diagram of exact solutions $u(x, 0.5, t)$ at $t = 0, 0.1, 0.2, \dots, 2$ for Example 2



solutions $u(x, 0.5, t)$ at many different time levels and different values of time fractional order i.e. α have been plotted in Fig. 3, while the corresponding exact solutions have been shown in Fig. 4. Furthermore, Table 1 shows the convergence with respect to time discretization.

Example 2 (Non-regular domain) In this example, we take again $\gamma_1 = \gamma_2 = 1$ and assume that

$$u(x, y, t) = t^3 \exp(x + y),$$

Table 2 The L_∞ error with fixed $N = 441$, $\alpha = 1.2$ and different time-steps for Example 2

t	$\Delta t = 0.1$	$\Delta t = 0.05$	$\Delta t = 0.01$
$t = 0.000000$	0.00000000	0.00000000	0.00000000
$t = 0.100000$	0.00148778	0.00104865	0.00022082
$t = 0.200000$	0.00547895	0.00264969	0.00048595
$t = 0.300000$	0.00800747	0.00358613	0.00066444
$t = 0.400000$	0.00899216	0.00411414	0.00077587
$t = 0.500000$	0.00941117	0.00435965	0.00083423
$t = 0.600000$	0.00935067	0.00434740	0.00084615
$t = 0.700000$	0.00882321	0.00408782	0.00081763
$t = 0.800000$	0.00780302	0.00358998	0.00075120
$t = 0.900000$	0.00630339	0.00286859	0.00064914
$t = 1.000000$	0.00435741	0.00192515	0.00051515

is the exact solution of the problem (1)–(3). Moreover, the domain of the problem is considered as

$$\Omega = \left\{ (x, y) : \left(x - \frac{1}{2}\right)^2 + 4\left(y - \frac{1}{2}\right)^2 \leq \frac{1}{4} \right\},$$

the approximation of this domain by different number of nodal points, while the regular distributed nodes are used for interior of the domain, are shown in Fig. 5.

The functions $\varphi(x, y)$, $\psi(x, y)$, and $g(x, y, t)$ are defined accordingly and also $f(x, y, t)$ is given by

$$f(x, y, t) = \frac{6t^{3-\alpha}e^{x+y}}{(\alpha^2 - 5\alpha + 6)\Gamma(2 - \alpha)} - 2t^3e^{x+y} + 3t^2e^{x+y}. \tag{55}$$

As previous example, Fig. 6 presents the absolute error of approximate MLPG solutions at different time levels with $\Delta t = 0.05$ and $N = 247$ for $\alpha = 1.2$. Also, the approximate MLPG solutions $u(x, 0.5, t)$ at many different time levels and different values of time fractional order i.e. α have been plotted in Fig. 7, while the corresponding exact solutions have been shown in Fig. 8. Moreover, Table 2 shows the convergence with respect to Δt .

Conclusions

In this paper, an efficient and accurate computational method namely meshless local Petrov–Galerkin (MLPG) method, which is based on the Galerkin weak form and moving least squares (MLS) approximation, has been applied to the time fractional two-dimensional diffusion-wave equation. The time fractional derivative has been defined by Caputo sense for $(1 < \alpha < 2)$. We have considered a arbitrary 2-D domain, which can be non-regular in general, while Dirichlet boundary conditions are prescribed to the boundaries of the domain. We have used meshless Galerkin weak form for the interior nodes whereas the meshless collocation technique has been applied to the nodes on the boundaries of the domain. As a consequence of imposing Dirichlet boundary conditions directly, the general domains are also applicable easily. In the proposed MLPG method, the moving least square (MLS) approximation has been used to construct shape functions which plays important rule in the convergence

and stability of the method. Two numerical experiments have been presented and satisfactory agreements are obtained.

Acknowledgements The author is very grateful to two anonymous reviewers for carefully reading the paper and for their comments and suggestions which have improved the paper very much.

References

1. Miller, K., Ross, B.: An Introduction to the Fractional Calculus and Fractional Differential Equations. Wiley, New York (1993)
2. Samko, S., Kilbas, A., Marichev, O.: Integrals and Derivatives of the Fractional Order and Some of Their Applications. Nauka i Tekhnika, Minsk (1987). (in Russian)
3. Bhrawy, A., Dohac, E., Baleanu, D., Ezz-Eldien, S.: A spectral tau algorithm based on Jacobi operational matrix for numerical solution of time fractional diffusion-wave equations. *J. Comput. Phys.* **293**, 142–156 (2015)
4. Heydari, M., Hooshmandasl, M., Ghaini, F.M., Cattani, C.: Wavelets method for the time fractional diffusion-wave equation. *Phys. Lett. A* **379**, 71–76 (2015)
5. Wang, K., Liu, S.: A new solution procedure for nonlinear fractional porous media equation based on a new fractional derivative. *Nonlinear Sci. Lett. A* **7**(4), 135–140 (2016)
6. Sayevand, K., K, P.: Analysis of nonlinear fractional KdV equation based on He's fractional derivative. *Nonlinear Sci. Lett. A* **7**(3), 77–85 (2016)
7. Liu, F.-J., Li, Z.-B., Zhang, S., Liu, H.-Y.: He's fractional derivative for heat conduction in a fractal medium arising in silkworm cocoon hierarchy. *Therm. Sci.* **19**(4), 1155–1159 (2015)
8. Belytschko, T., Lu, Y.Y., Gu, L.: Element-free Galerkin methods. *Int. J. Numer. Methods Eng.* **37**(2), 229–256 (1994)
9. Belytschko, T., Lu, Y.Y., Gu, L.: Element free Galerkin methods for static and dynamic fracture. *Int. J. Solids Struct.* **32**, 2547–2570 (1995)
10. Liu, G., Gu, Y.: An Introduction to Meshfree Methods and Their Programming. Springer, Berlin (2005)
11. Kansa, E.: Multiquadrics—a scattered data approximation scheme with applications to computational fluid-dynamics. I. Surface approximations and partial derivative estimates. *Comput. Math. Appl.* **19**(8–9), 127–145 (1990)
12. Dehghan, M., Shokri, A.: A numerical method for solution of the twodimensional sine-Gordon equation using the radial basis functions. *Math. Comput. Simul.* **79**, 700–715 (2008)
13. Abbasbandy, S., Ghehsareh, H.R., Hashim, I.: A meshfree method for the solution of two-dimensional cubic nonlinear Schrödinger equation. *Eng. Anal. Bound. Elem.* **37**(6), 885–898 (2013)
14. Parand, K., Hemami, M.: Numerical study of astrophysics equations by meshless collocation method based on compactly supported radial basis function. *Int. J. Appl. Comput. Math.* 1–23 (2016). doi:10.1007/s40819-016-0161-z
15. Fu, Z.-J., Chen, W., Ling, L.: Method of approximate particular solutions for constant- and variable-order fractional diffusion models. *Eng. Anal. Bound. Elem.* **57**, 37–46 (2015)
16. Fu, Z.-J., Chen, W., Yang, H.-T.: Boundary particle method for Laplace transformed time fractional diffusion equations. *J. Comput. Phys.* **235**, 52–66 (2013)
17. Chen, W., Ye, L., Sun, H.: Fractional diffusion equations by the Kansa method. *Comput. Math. Appl.* **59**(5), 1614–1620 (2010)
18. Shivanian, E.: A new spectral meshless radial point interpolation (SMRPI) method: a well-behaved alternative to the meshless weak forms. *Eng. Anal. Bound. Elem.* **54**, 1–12 (2015)
19. Shivanian, E.: Spectral meshless radial point interpolation (smrpi) method to two-dimensional fractional telegraph equation. *Math. Methods Appl. Sci.* **39**(7), 1820–1835 (2016)
20. Aslefallah, M., Shivanian, E.: Nonlinear fractional integro-differential reaction–diffusion equation via radial basis functions. *Eur. Phys. J. Plus* **130**(3), 1–9 (2015)
21. Fatahi, H., Saberi-Nadjafi, J., Shivanian, E.: A new spectral meshless radial point interpolation (SMRPI) method for the two-dimensional fredholm integral equations on general domains with error analysis. *J. Comput. Appl. Math.* **294**, 196–209 (2016)
22. Shivanian, E.: A meshless method based on radial basis and spline interpolation for 2-D and 3-D inhomogeneous biharmonic bvps. *Z. Naturforschung A* **70**(8), 673–682 (2015)
23. Abbasbandy, S., Shivanian, E.: Numerical simulation based on meshless technique to study the biological population model. *Math. Sci.* **10**(3), 123–130 (2016)

24. Gu, Y., Liu, G.: A boundary radial point interpolation method (BRPIM) for 2-D structural analyses. *Struct. Eng. Mech.* **15**, 535–550 (2003)
25. Liu, G., Yan, L., Wang, J., Gu, Y.: Point interpolation method based on local residual formulation using radial basis functions. *Struct. Eng. Mech.* **14**, 713–732 (2002)
26. Liu, G., Gu, Y.: A local radial point interpolation method (LR-PIM) for free vibration analyses of 2-D solids. *J. Sound Vib.* **246**(1), 29–46 (2001)
27. Dehghan, M., Ghesmati, A.: Numerical simulation of two-dimensional sine-Gordon solitons via a local weak meshless technique based on the radial point interpolation method (RPIM). *Comput. Phys. Commun.* **181**, 772–786 (2010)
28. Shivanian, E.: Analysis of meshless local radial point interpolation (MLRPI) on a nonlinear partial integro-differential equation arising in population dynamics. *Eng. Anal. Bound. Elem.* **37**(12), 1693–1702 (2013)
29. Shivanian, E.: Analysis of meshless local and spectral meshless radial point interpolation (MLRPI and SMRPI) on 3-D nonlinear wave equations. *Ocean Eng.* **89**, 173–188 (2014)
30. Shivanian, E., Khodabandehlo, H.R.: Meshless local radial point interpolation (MLRPI) on the telegraph equation with purely integral conditions. *Eur. Phys. J. Plus* **129**(11), 1–10 (2014)
31. Shivanian, E.: On the convergence analysis, stability, and implementation of meshless local radial point interpolation on a class of three-dimensional wave equations. *Int. J. Numer. Methods Eng.* **105**(2), 83–110 (2016)
32. Hosseini, V.R., Shivanian, E., Chen, W.: Local integration of 2-D fractional telegraph equation via local radial point interpolant approximation. *Eur. Phys. J. Plus* **130**(2), 1–21 (2015)
33. Shivanian, E., Khodabandehlo, H.R.: Application of meshless local radial point interpolation (MLRPI) on a one-dimensional inverse heat conduction problem. *Ain Shams Eng. J.* **7**(3), 993–1000 (2016)
34. Shivanian, E., Rahimi, A., Hosseini, M.: Meshless local radial point interpolation to three-dimensional wave equation with neumann's boundary conditions. *Int. J. Comput. Math.* 1–17 (2015). doi:[10.1080/00207160.2015.1085032](https://doi.org/10.1080/00207160.2015.1085032)
35. Hosseini, V.R., Shivanian, E., Chen, W.: Local radial point interpolation (MLRPI) method for solving time fractional diffusion-wave equation with damping. *J. Comput. Phys.* **312**, 307–332 (2016)
36. Atluri, S., Zhu, T.: A new meshless local Petrov–Galerkin (MLPG) approach in computational mechanics. *Comput. Mech.* **22**, 117–127 (1998)
37. Atluri, S., Zhu, T.: A new meshless local Petrov–Galerkin (MLPG) approach to nonlinear problems in computer modeling and simulation. *Comput. Model. Simul. Eng.* **3**(3), 187–196 (1998)
38. Atluri, S., Zhu, T.: New concepts in meshless methods. *Int. J. Numer. Methods Eng.* **13**, 537–556 (2000)
39. Atluri, S., Zhu, T.: The meshless local Petrov–Galerkin (MLPG) approach for solving problems in elastostatics. *Comput. Mech.* **25**, 169–179 (2000)
40. Dehghan, M., Mirzaei, D.: The meshless local Petrov–Galerkin (MLPG) method for the generalized two-dimensional non-linear Schrödinger equation. *Eng. Anal. Bound. Elem.* **32**, 747–756 (2008)
41. Dehghan, M., Mirzaei, D.: Meshless local Petrov–Galerkin (MLPG) method for the unsteady magnetohydrodynamic (MHD) flow through pipe with arbitrary wall conductivity. *Appl. Numer. Math.* **59**, 1043–1058 (2009)
42. Gu, Y., Liu, G.: A meshless local Petrov–Galerkin (MLPG) method for free and forced vibration analyses for solids. *Comput. Mech.* **27**, 188–198 (2001)
43. Shirzadi, A., Sladek, V., Sladek, J.: A local integral equation formulation to solve coupled nonlinear reaction–diffusion equations by using moving least square approximation. *Eng. Anal. Bound. Elem.* **37**, 8–14 (2013)
44. Shivanian, E.: Meshless local Petrov–Galerkin (MLPG) method for three-dimensional nonlinear wave equations via moving least squares approximation. *Eng. Anal. Bound. Elem.* **50**, 249–257 (2015)
45. Shivanian, E., Abbasbandy, S., Alhuthali, M.S., Alsulami, H.H.: Local integration of 2-D fractional telegraph equation via moving least squares approximation. *Eng. Anal. Bound. Elem.* **56**, 98–105 (2015)
46. Shivanian, E.: Local integration of population dynamics via moving least squares approximation. *Eng. Comput.* **32**(2), 331–342 (2016)
47. Hu, D., Long, S., Liu, K., Li, G.: A modified meshless local Petrov–Galerkin method to elasticity problems in computer modeling and simulation. *Eng. Anal. Bound. Elem.* **30**, 399–404 (2006)
48. Liu, K., Long, S., Li, G.: A simple and less-costly meshless local Petrov–Galerkin (MLPG) method for the dynamic fracture problem. *Eng. Anal. Bound. Elem.* **30**, 72–76 (2006)